19th Brazilian Congress of Thermal Sciences and Engineering
November 6th–10th, 2022, Bento Gonçalves - RS - Brazil

ENC-2022-0481
EXPERIMENTAL EVALUATION OF A HYBRID PHOTOVOLTAIC-THERMAL SYSTEM WITH GLYCEROL-BASED PHASE CHANGE MATERIAL

Marco Antonio Bertogna
Stephan Hennings Och
José Viriato Coelho Vargas
Postgraduate Program in Mechanical Engineering (PGMEC), Federal University of Paraná (UFPR), Curitiba, PR, Brazil
marco.bertogna@ufpr.br, stephan.och@ufpr.br, viriato@ufpr.br

Luís Mauro Moura
Pontifícia Universidade Católica do Paraná, Mechanical Engineering Graduate Program, Curitiba, PR, Brazil
Department of Mechanical Engineering - UFPR - Curitiba, PR, Brazil
luis.moura@pucpr.br

Abstract. *The temperature rise of a photovoltaic cell provokes a reduction of it's electric efficiency. Options of cooling the cells include hybrid photovoltaic-thermal (PVT) solar system and using phase change materials (PCMs). These two systems work well together, increasing each other's efficiency. Commercially available PCMs are expensive, reducing their viability. In this research, a PVT-PCM system is analysed, using a glycerol-based PCM, which is a byproduct of bio-diesel production. Outdoor experiments are made to compare this system's performance against a standard PV panel. Tests are held in a city with mild weather to test the PCM's viability. A mathematical model is proposed, validated and used to determine the system's viability in a hot desert climate. It was found that, during the winter, the use of a cooling system is not required even in a clear sunny day, but the thermal system provides useful thermal energy. Simulation of the system in the Nevada desert showed that the cooling system is not sufficient for too harsh climates and changes to the composition of the system are proposed.*

Keywords: *Hybrid Photovoltaic/Thermal System, Phase Change Material, Glycerol, Temperature Control, Outdoor Evaluation*

1. INTRODUCTION

Due to ever-growing concerns with environmental issues, the search for renewable energy sources has steadily grown in the past decades. Solar photovoltaic cells have seen a massive growth, from an worldwide installed base of 1 Gigawatt of power (GWp) in 2004 to 627 GWp in 2019 (Detollenaere *et al.*, 2020). These cells have the downside of having it's electrical efficiency reduced as it's temperature increases. That loss is estimated in 0.4% for every 1 K above the Normal Operating Cell Temperature (NOCT) for the case of crystalline silicon cells (Mau and Jahn, 2006).In order to avoid that loss, there's ongoing research on methods of reducing the operating temperature of the cells and harnessing the energy that would be dissipated. One of these methods consists of a hybrid photovoltaic-thermal system (PVT), in which a cooling fluid extracts energy from the cell, providing useful thermal energy. Phase-change materials (PCMs) have also been employed to absorb the cell's energy, storing it in the form of latent heat.

The combination of both systems (resulting in a system that shall be called PVT+PCM) is explored, due to their symbiotic nature.Browne *et al.* (2015) compared a PVT and PVT+PCM system, finding that the heat storage potential grows up to 100% when incorporating the PCM in the hybrid system, with an average temperature increase of 6°C. The time in which the energy is available also saw an increase of 100%, due to the energy released by the PCM during the night. Fayaz *et al.* (2019) did both a numerical and an experimental analysis of a PVT+PCM system, achieving an increase in electrical output of 9.2% and 12.75%, when comparing a PV with a PVT and PVT+PCM, respectively. The peak temperature using a 0.5 LPM (liters per minute) water flow was 75°C and 69°C for the PVT and PVT+PCM systems, respectively. When increasing the water flow, the maximum temperature dropped significantly when using 1 LPM, reaching 70°C and 64°C. For flows higher than that the peak temperature drop wasn't as significant.

The capacity of heat storage per volume of a PCM is 5-14 times higher than the capacity of materials using sensible storage, such as water (Sharma *et al.*, 2009). The downsides of using them include high cost(Islam *et al.*, 2016) and low thermal conductivity, especially on organic ones (Jebasingh, 2016). Attempts to make PCMs more viable include the addition of materials to increase it's thermal properties and testing alternative substances as PCMs.

Hendricks and Van Sark (2013) studied a PV+PCM system in the Netherlands utilizing commercially available PCMs. The study showed that the increase in electrical energy output was 3%, showing that utilizing a PCM alone is not sufficient to warrant it's cost, and a mean of extracting thermal energy is needed. Malvi *et al.* (2011) studied the relation of a PCM reservoir and it's heat storage capacity. There was a considerable increase in the capacity up to 15 mm thickness. Diminishing returns were found from 15 mm to 25 mm and up to 30 mm the increase was even smaller. There were no benefits seen for thicknesses over 30 mm. The difference in electricity output between 0 and 30 mm was 6.5%.

In order to increase organic PCMs' thermal conductivity, the viability of incorporating other materials in them is studied. Tests with a graphite-PCM composite material using 5% in weight (%wt) of exfoliated graphite in it's flake and amorphous forms showed a decrease of 3.4% and 21% in the melting latent heat, respectively. The thermal conductivity was increased in 14.1% and 12.1% (Jebasingh, 2016). Incorporating 5% of volume of graphene sponge into fatty amine PCMs resulted in an increase of 164.4%-176.7% to their thermal conductivity (Chen *et al.*, 2020) .

Ahmadi *et al.* (2021) made an analysis of a PV system utilizing a composite paraffin PCM+PS-CTN foam with the following configurations: PVT; PV+PCM; PV+composite; PVT+PCM; PVT+composite. The PVT+composite system wielded the highest energy efficiency and the use of active water cooling was beneficial for both passive systems (standard PCM as well as composite), while the passive systems increased the span in which the active system could provide thermal energy, showcasing the synergy of the components in a PVT+PCM system. Rad *et al.* (2021) tested a PVT+PCM system with a water-based thermal system and a salt hydrate PCM. The system was tested with and without an aluminum fin porous material incorporated to the PCM. The maximum temperature during the test was 80°C for a conventional PV cell with a drop of 30.6% and 36.5% for the systems without and with the porous aluminum fins, respectively.

Fins can be used to improve the thermal conductivity between components. Zhao *et al.* (2022) studied the effect of different numbers and widths of aluminum fins between PV module and PCM. The melting time of the PCM was reduced (thus, showing that it was able to extract more heat from the PV module) as the length of the fins increased. There was a shift in behaviour for fins longer than 25 mm in both cases studied (3 sparse fins and 12 tight ones), for the first case, the melting time became constant, indicating no improvement after that point. For the tightly packed fins, there was still an improvement, albeit reduced. As for the distance, a pitch (spacing) of 7.5mm was found optimal, with a melting time over 10% lower than when using a 5 mm pitch and 20% lower than 20 mm. In all cases, the fins were kept as 5% of the volume of the reservoir.

Glycerol, a byproduct of bio-diesel's production chain, has been studied as an alternative PCM. In order to change it's melting point for a suitable temperature, glycerol is merged with fatty acids, forming an ester with thermal properties shown in Tab. 1. To increase the thermal conductivity (k) of the PCMs, 5%wt of expanded graphite (EG) was added. (Sarı *et al.*, 2010)

Table 1. Thermal properties of glycerol-fatty acid esters (Sarı *et al.*, 2010)

Material	Melting point (°C)	Latent heat (kJ/kg)	k (W/m K)	k using EG (W/m K)
Glycerol trimyristate	31.96	154.3	0.23	0.29
Glycerol tripalmitate	58.50	185.9	0.19	0.27
Glycerol tristearate	63.45	149.4	0.17	0.19

Osaka (2019) proposed a system utilizing a PVT+PCM system with a glycerol-based PCM. Using water as the active coolant and fins to improve the thermal conductivity between the panel and the PCM. Since this is not a pure substance, it does not have an specific melting point. Analysis of the substance in a calorimeter showed that it completely melted after reaching 42°C, which is a good temperature considering the operating range of a PV system. The system was tested in three conditions: With 0.026 l/s water flow, 0.014 l/s flow and no flow. There was no noticeable difference between the first two cases, with both producing 3% more tension than the third. The maximum heat difference when comparing the PVT+PCM system with a PV was 9.6°C. The test was made in an indoor lab, with a constant irradiance of 1000 Wm^{-2}.

In this paper, this system will be analysed once more, now in an outdoor environment. The goal is to observe the effects different weather conditions have in the production of energy and how well this cooling system manages the temperature of the module in the city of Curitiba, located in southern Brazil with an oceanic temperate climate (cfb). It is a city with mild climate, where the hottest month (January) has an average peak temperature of 27.1°C and the highest temperature ever recorded being 35.5°C (Inmet, 2022). The average total daily irradiation in January 2017 was 5318 Wh/m^2 (Pereira *et al.*, 2017). Due to glycerol's poorer thermal properties when compared to other PCMs (paraffin, for instance) it shall be determined if it is deemed a viable PCM alternative for places with such conditions.

2. METHODOLOGY

The aforementioned system constructed by Osaka (2019) consists of a 10 W crystalline PV module, a reservoir containing the glycerol-based PCM and a thermal system in which water flows and exchange heat with the PCM. In this section will be discussed the assembly of the system and the approach to measurement of the properties.

The system is placed on the rooftop, as shown in Fig. 1. The panels are pointed towards the geographic north, in order to maximize the average yearly electricity production. The system is built with the following configuration, from top to bottom, as shown in Fig. 2: PV module, PCM reservoir and thermal system. An aluminum plate with 7 fins with a 25 mm pitch and 18 mm height is placed between the PV panel and the PCM for an improved heat conductivity.

Figure 1. Layout of the system

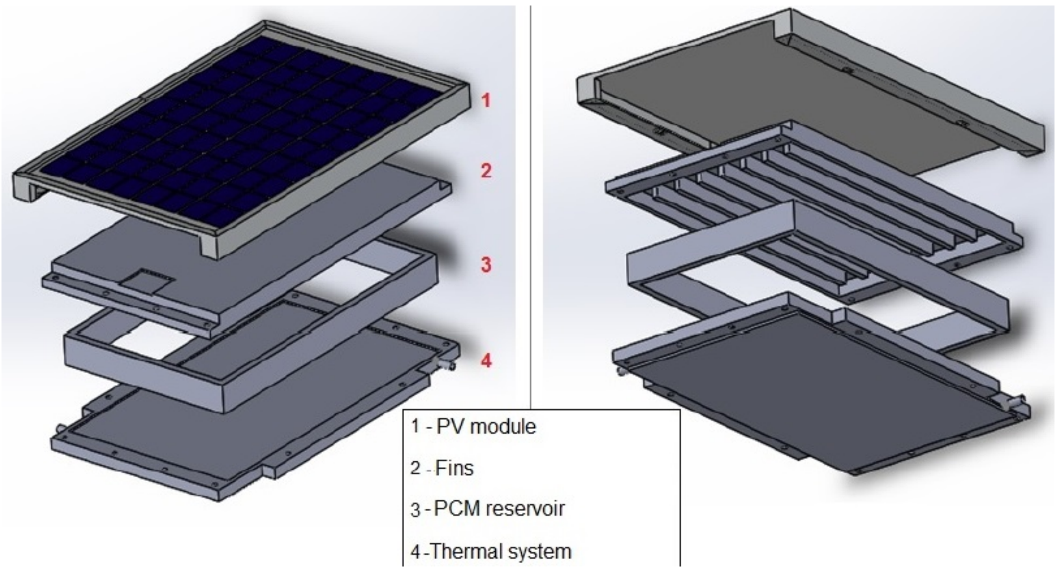

Figure 2. Layout of the components (Osaka, 2019)

The glycerol-based PCM is inserted into a 30 mm deep reservoir in it's solid form and melted with a heat gun until the reservoir is completely filled. Figure 3 shows the process of filling the reservoir, as well as the fins used between the PCM and the panel. The thermal system consists in a canal with 8 mm depth and the length of the panel, where water is pumped from and to a 10 liters reservoir with a flow of 0.014 l/s through the use of an aquarium pump.

(a) (b)

Figure 3. (a) Reservoir being filled with solid PCM, fins and thermocouples at the back. (b) Filled reservoir.

The temperature of the PV cells, the fins, the PCM and and the water, as well as ambient temperature, are measured with type T thermocouples. For the water, the temperature of the entrance and exit are measured and an average between them is used for calculations. The data is sent to a data acquisition device, which also stores the open circuit voltage (OCV) of the cells. A Kipp and Zonen CMP11 pyranometer is used to measure the global solar irradiance I (W/m^2).

The electrical efficiency (η_e) of the system shall be analysed by Eq. 1, provided to this panel's model, with T_0 being 24°C. If the panel's temperature is lower than that, the efficiency does not increase past 17%. The thermal energy (Q_t provided by the heated water, shown in Eq.2, is given through water's heat capacity multiplied by the temperature difference between it and the ambient. C_w is the water's heat capacity (J/K), T_{pv}, T_a and T_w are the temperatures of the PV panel, the ambient and the water, respectively, in °C.

$$\eta_e = 0.17(1 - 0.0405(T_{pv} - T_0)) \tag{1}$$

$$Q_t = C_w(T_w - T_a) \tag{2}$$

3. MATHEMATICAL MODEL

A thermal resistance circuit is used to model the system, as shown in Fig. 4. Energy enters the system through the irradiance represented by the blue arrow, with losses caused by the panel's absorptivity and the protective glass' transmittance. It is then used for electricity production with an efficience of η(upward arrow). The remaining energy is dissipated to the ambient and the PCM/thermal system. The symbols in the picture are explained in Tab. 2. The U symbols represent the global heat transfer coefficient and the description in the table refers to which component are analysed. U_3 and U_4 are both between the aluminum fins and the PCM, but are detached for simplicity since the fins' properties remain constant whereas the PCM's change according to it's phase.

Through the equation derived from the first law of thermodynamics (Eq. 3). It is possible to determine the variation of temperature for the components of the PVT+PCM system through the day, by applying an energy balance to each of them (Eq. 4-6). These equations are solved using a fourth order Runge-Kutta method with time steps of 60s. A and C are the values of the components areas and heat capacities, respectively.

$$\frac{dE}{dt} = mc_p\frac{dT}{dt} = \dot{E}_{in} - \dot{E}_{out} + \dot{E}_{gen} \tag{3}$$

$$\frac{dT}{dt}_{pv} = [(\alpha\tau - \eta)I - U_1(T_{pv} - T_a) - U2(T_{pv} - T_{al})]\frac{A_{pv}}{C_{pv}} \tag{4}$$

$$\frac{dT}{dt}_{pcm} = \left[\frac{U_3U_4}{U_3 + U_4}(T_{al} - T_{pcm}) - U_5(T_{pcm} - T_w)\right]\frac{A_b}{C_{pcm}} \tag{5}$$

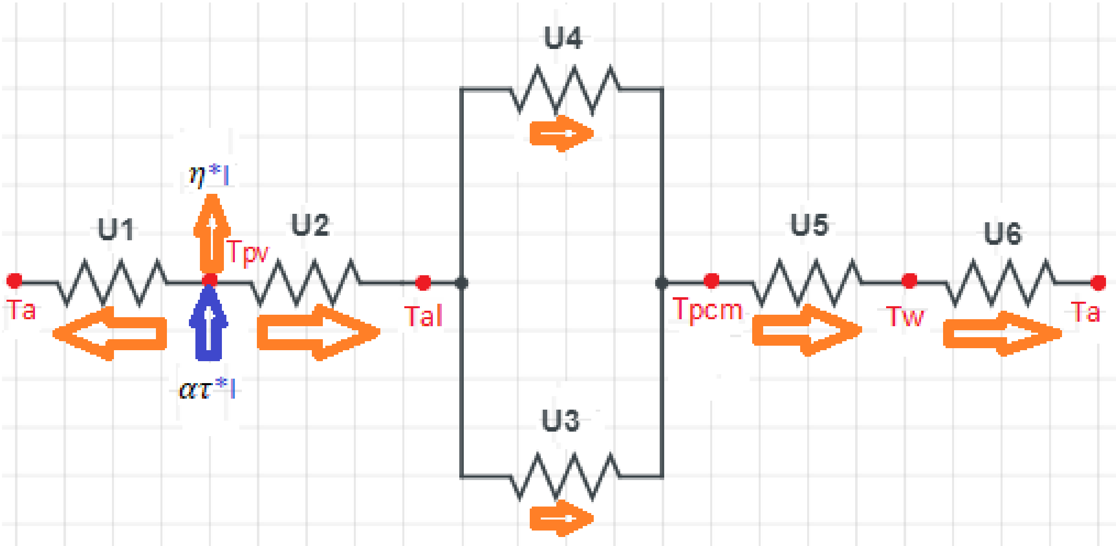

Figure 4. Representation of the thermal circuit

Table 2. Meaning of symbols used in the thermal circuit

Temperatures		Heat transfer coefficient		Miscellaneous	
Symbol	Meaning	Symbol	Meaning	Symbol	Meaning
Ta	Ambient temperature	U_1	PV-ambient	I	Irradiance
Tpv	PV temperature	U_2	PV-fins	α	Absorptivity
Tal	fin temperature	U_3	fins-PCM	τ	Transmittance
Tpcm	PCM temperature	U_4	fins-PCM	η	electrical efficiency
Tw	Water temperature	U_5	PCM-water		
		U_6	Water-ambient		

$$\frac{dT}{dt}_w = [U_5(T_{pcm} - T_w) - U_6(T_w - T_a)]\frac{A_b}{C_w} \tag{6}$$

The global heat transfer constants were found through the use of the least squares method and considered constant throughout the simulation. The comparison between the values found experimentally and through the simulation are shown in Fig. 5. The parameters related to the PCM had two instances, one for each phase and the transition point was set at 40°C with satisfying results. This model now grants the possibility of studying the system in different conditions and shall be used to analyse how the system fares in a city with extreme weather conditions. It was chosen to compare it with a hot summer day in Las Vegas, situated in the Nevada desert, with it's irradiance and ambient temperature provided by America's National Renewable Energy Laboratory (Stoffel and Andreas, 2006). The total global irradiation of the chosen day was 9047 Wh/m^2, 70% higher than Curitiba's January average. Through the same source, a spring day with 6210 Wh/m^2 global irradiation (15% higher than the January average) is used to simulate the conditions of Curitiba's summer peak.

4. RESULTS AND DISCUSSION

Data for temperature and irradiance were retrieved for a cloudy and a sunny day in June, approaching winter. Figure 6-a shows the temperatures of the panels on a cloudy day, as well as the irradiance level. Irradiance levels sparked when the sun briefly showed through the clouds. The temperature of the PVT+PCM system was higher at times, due to it receiving energy from the PCM, resulting in a slower cooling than the PV system. However, the impact of the temperature increase of either system toward it's electrical output is negligible, barely going above ambient temperature. Figure 6-(b) shows the temperature of the components throughout the day, in some instances the temperature of the PCM is higher than the PV panel, due to gusts of wind naturally cooling the panel. This corroborates with the reasoning for the PVT+PCM system's panel having a higher temperature than the PV panel.

A comparison was made with the mathematical model for the cloudy day data, as seen in Fig. 7-(a). There was a considerable discrepancy between the results for both the water and panel. For the first, it can be attributed to the water reservoir being warmed by the floor and through the energy received by the sun and the water pump, whereas in the laboratory where the model was conceived, the water reservoir remained isolated. As for the panel, the difference can be

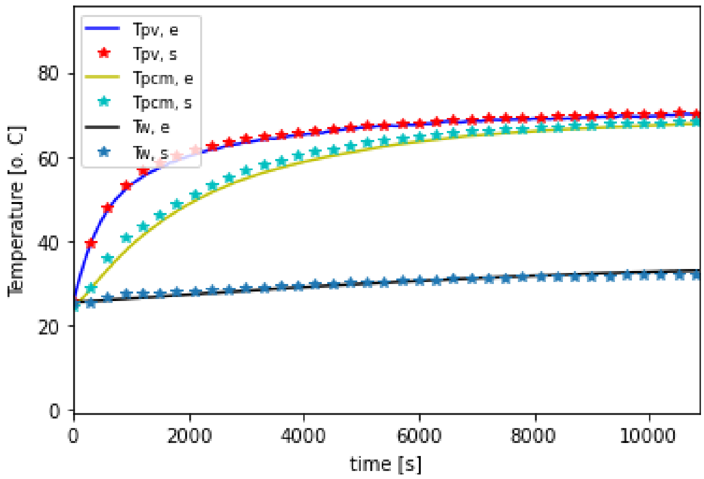

Figure 5. Comparison between experimental values (e) and simulation (s) of the components' temperatures

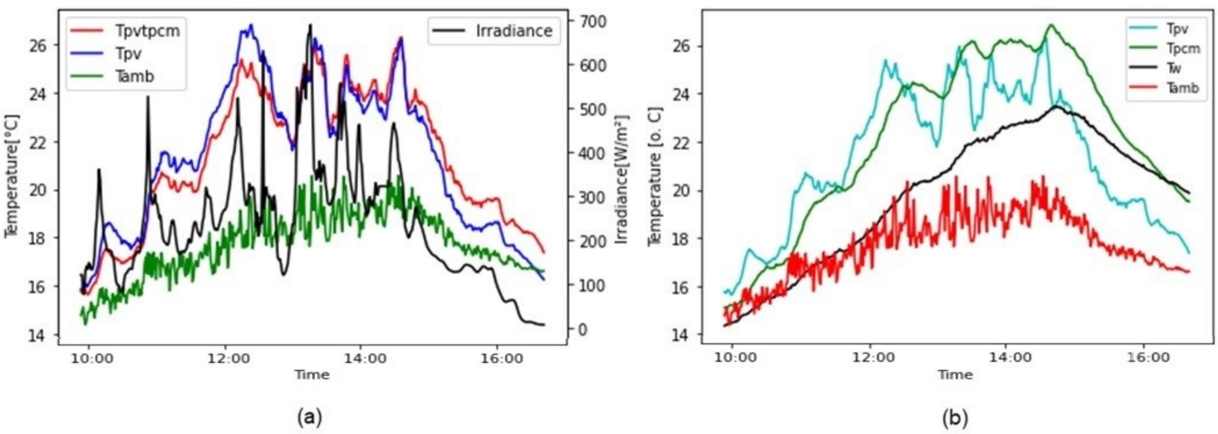

Figure 6. a) Irradiance and temperature of the panels on a cloudy day b) Temperature of PVT-PCM components on a cloudy day

attributed to the cooling caused by the wind, since the mathematical model was made using a constant 1 m/s wind speed. Fig. 7-(b) shows the result when multiplying the heat exchange between the panel and the ambient (U_1) by 1.5, with the model's PV temperature being considerably closer to the experimental when compared to Fig. 7-(a). The average error went from 3.4°C to 2.1°C. Raising U_1's value reduced the system's top temperature in 3.9°C and the average in 2.5°C, indicating the importance of wind to naturally cooling a PV system. For better accuracy, U_1 can be computed with the convection model for a flat plate, as shown in Eq. 7 (Bejan, 2013). h stands for the convective heat transfer coefficient, k for the thermal conductivity and Pr to the Prandtl number for the air, while L_p is the length of the panel and Re is Reynolds' number. For the model to be used, the wind speed also needs to be measured.

$$U_1 = h_a = 0.664 \frac{k_a Pr^{1/3}}{Lp} Re_L^{0.5} \tag{7}$$

Data for a sunny day is shown in Fig. 8. The test was finished when the irradiance level started to steeply decline. It shows that, despite being a clear sunny day, the temperature of the panels during the winter doesn't increase much, reaching a peak of 33°C for both of them. The PCM's low temperature during the morning helped the PVT+PCM panel to sustain a lower temperature than the PV panel, but strong winds around 11:30 am brought both to the same temperature. The irradiance level for a sunny day follows a parabolic distribution, allowing it to be interpolated with good precision from a set of acquired data points, unlike for a cloudy day, where the irradiance level is unstable.

Figure 9 shows the temperature of both panels for a cloudy (c) and a sunny (s) day from 6:30 am to midnight as well as the difference between the water temperature and ambient temperature ($\Delta T = T_w - T_a$), which is used to determine the amount of thermal energy the system is able to provide. It also shows the open-circuit voltage for both cases. The temperature of no panel has risen significantly above 24°C, meaning that their electrical efficiency is not reduced through the day, and the Voc for all cases plateaued at the same level. Corroborating with the notion that thermal management

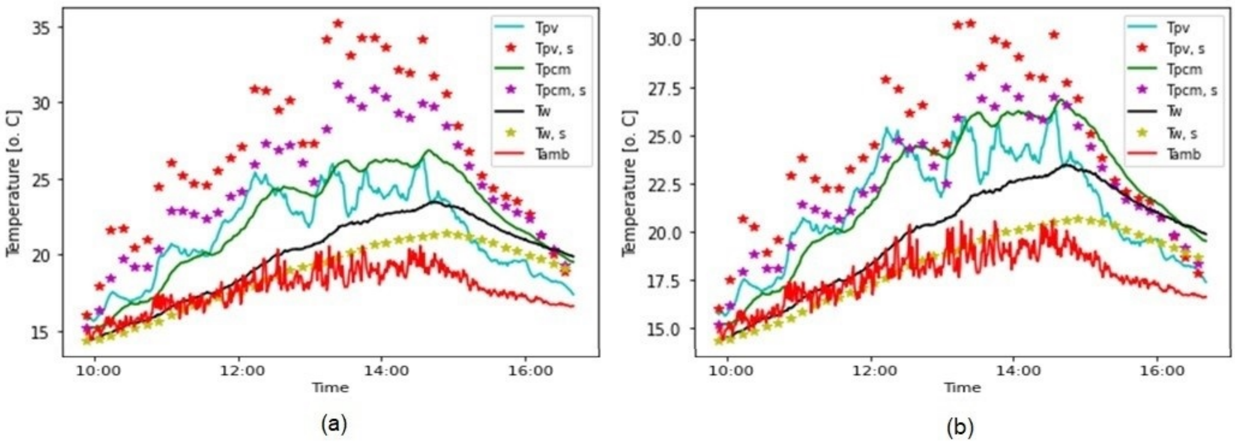

Figure 7. a) Comparison between the experimental and numerical temperatures for a foggy day. b) comparison for when U_1 is increased by 50%

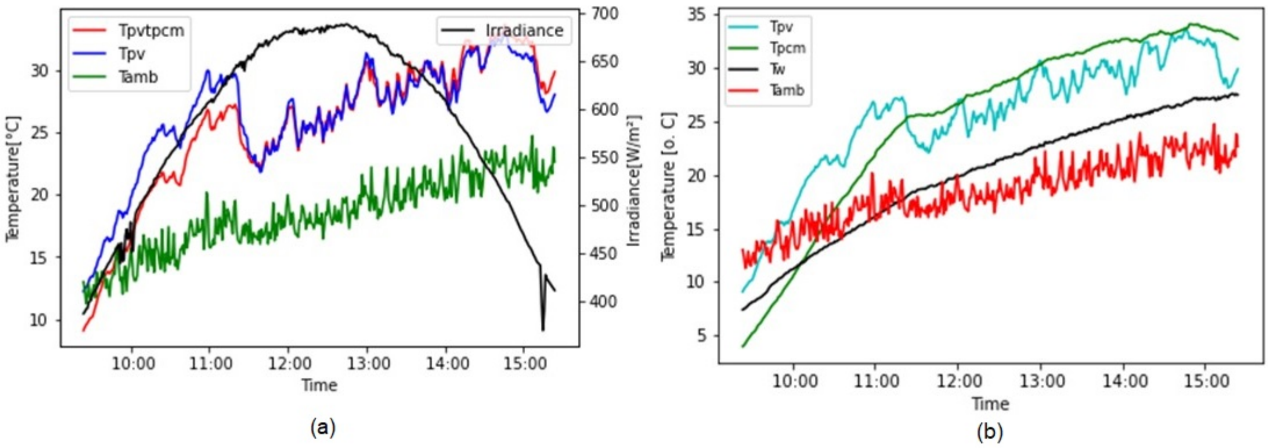

Figure 8. a) Irradiance and temperature of the panels on a sunny day b) Temperature of PVT+PCM components on a sunny day

is not required in cold weather, such as studied in the Netherlands (Hendricks and Van Sark, 2013). Most of the studies shown in the introductory section 1 were held in places hot climates such as the Middle East and Southern Asia, where the operating temperature of the panels is high.

The difference between water and ambient temperatures was considerably higher in a sunny day, reaching a peak of 5.6°C and providing up to 15 kJ of energy in a minute (though part of it is due to the water reservoir also being heated by the sun) through the use of Eq.2 with C_w being found as 3031.31 J/k through the use of least squares in section 3. For a cloudy day it peaked at 2.2°C and stayed at a much lower level throughout the day. The use of thermal energy is specially important during the winter, becoming the main point of implementing the system for cold seasons.

When utilizing the model to simulate the conditions in Las Vegas, days with small average wind speed were chosen, in order to mitigate the effects above mentioned. Figure 10-(a) shows the temperature for the three components throughout the summer day, with the panel peaking at almost 90°C. Rad *et al.* (2021) studied a PV system in Iran with as harsh of a weather and the panel's temperatures rose above 80°C, indicating that this is a plausible temperature. The PCM temperature quickly catches up with the PV module, which is expected since it's melting point is around ambient temperature. Figure 10-(b) shows a marginal gain when compared to the PV system, mostly due to the water flow. For the system to be viable in such conditions, a PCM with a higher melting point must be used. For the temperature to drop to reasonable levels, the use of a much stronger cooling system is required, but, by that point, alternatives such as a concentration-based solar system should be considered instead of a PV system or the use of a PV system made with materials with a lower temperature-related efficiency drop than crystalline silicon. Such systems are already employed in the Nevada desert, with projects such as the Nevada Solar One having a 64 MW nominal capacity.

The analysis of the milder day brings the results shown in Fig. 11. In this case it also shows the PV and PCM temperatures are similar, with the water temperature lagging behind. The average temperature difference between the PV and PVT+PCM system up to the point where they start cooling down was 3.5°C, which roughly translates to an increase

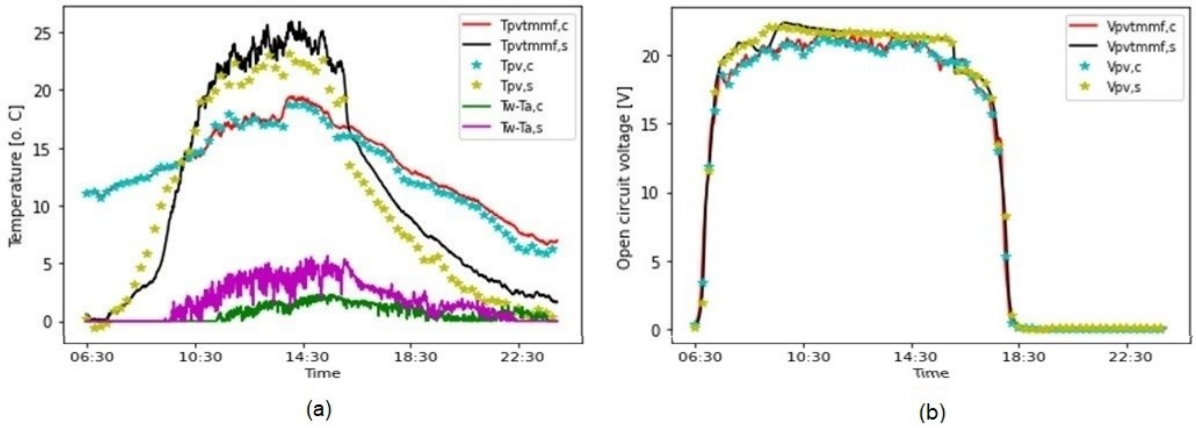

Figure 9. a) Comparison between the temperature of the panels and difference between water and ambient temperature in both scenarios b) Voc for both panels for both scenarios

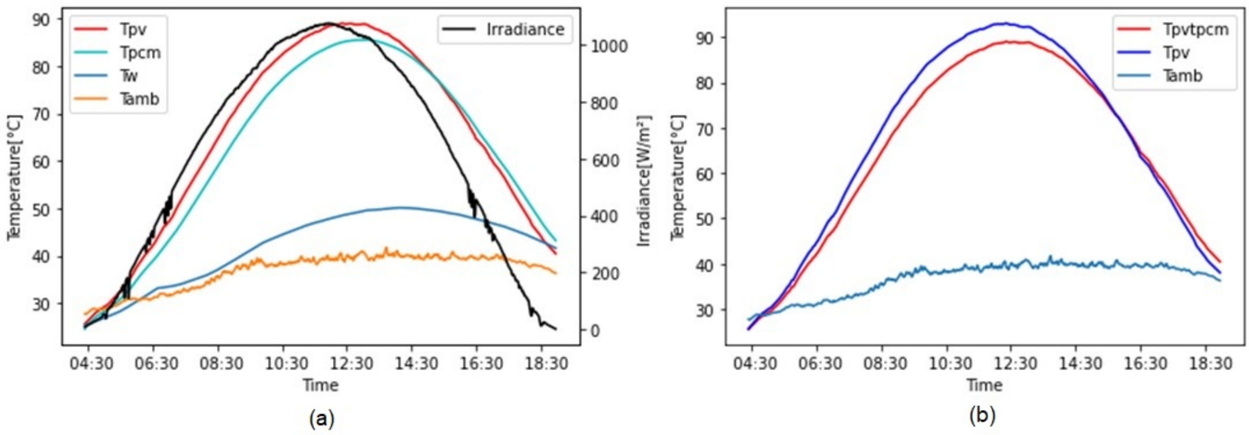

Figure 10. a) Temperature of PVT+PCM components and irradiance level - Las Vegas 18/06/2013 b)Temperature of PV and PVT+PCM panels - Las Vegas 18/06/2013

in electrical efficiency of 1.5%. The difference's peak was 5.3°C, considerably lower than the systems presented in section 1. For the system to be more effective, changes should be made. Swapping the disposition of the PCM and the thermal system could be beneficial for the cooling, with the downside of providing less thermal energy at night (since the PCM's temperature would become lower). An augmented water flow should be paired with the placement swap. Changes to the PCM system can also be made, with the employment of a porous structure or use of graphene, as seen in section 1 or by enlarging the depth of the reservoir and altering the structure of the aluminum fins.

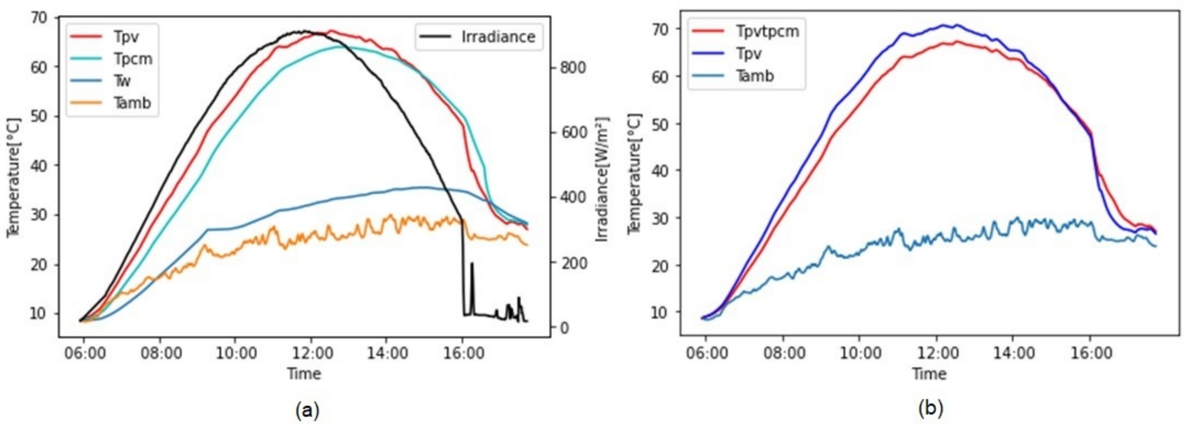

Figure 11. a) Temperature of PVT+PCM components and irradiance level - Las Vegas 14/03/2014 b) Temperature of PV and PVT+PCM panels - Las Vegas 14/03/2014

5. CONCLUSION

With the results acquired in section 4, it is possible to conclude that the usage of a cooling system is not required for a cloudy day, due to the small difference between the temperature of the panels and the ambient. Alterations should be made to the mathematical model in order to account for the outdoor conditions (varying wind speed and heating of the water reservoir). During the sunny day the temperature of the panels also barely rose, showing that for places with cold climates a cooling system for the panel is not needed. However, through the use of a thermal system it is shown that thermal energy can be extracted during the winter and the cooling system would come into action in summer/spring.

The analysis for the conditions with Las Vegas' summer peak showed that this cooling system is not robust enough to keep the panel's temperature low, nor is the PCMs melting point suitable. When using Las Vegas' spring data to simulate Curitiba's summer peak, the PVT+PCM system did not sustain a temperature much lower than the conventional PV system. Thus, alterations to the system must be considered.

6. REFERENCES

Ahmadi, R., Monadinia, F. and Maleki, M., 2021. "Passive/active photovoltaic-thermal (pvt) system implementing infiltrated phase change material (pcm) in ps-cnt foam". *Solar Energy Materials and Solar Cells*, Vol. 222, p. 110942.

Bejan, A., 2013. *Convection heat transfer*. John wiley & sons, 4th edition.

Browne, M.C., Lawlor, K., Kelly, A., Norton, B. and Mc Cormack, S.J., 2015. "Indoor characterisation of a photovoltaic/thermal phase change material system". *Energy Procedia*, Vol. 70, pp. 163–171.

Chen, T., Liu, C., Mu, P., Sun, H., Zhu, Z., Liang, W. and Li, A., 2020. "Fatty amines/graphene sponge form-stable phase change material composites with exceptionally high loading rates and energy density for thermal energy storage". *Chemical Engineering Journal*, Vol. 382, p. 122831.

Detollenaere, A., Van Wetter, J., Masson, G., Kaizuka, I., Jäger-Waldau, A. and Donoso, J., 2020. "Snapshot of global pv markets 2020 pvps task 1 strategic pv analysis and outreach". doi:10.13140/RG.2.2.24096.74248.

Fayaz, H., Rahim, N., Hasanuzzaman, M., Nasrin, R. and Rivai, A., 2019. "Numerical and experimental investigation of the effect of operating conditions on performance of pvt and pvt-pcm". *Renewable Energy*, Vol. 143, pp. 827–841.

Hendricks, J.H.C. and Van Sark, W.G.J.H.M., 2013. "Annual performance enhancement of building integrated photovoltaic modules by applying phase change materials". *Progress in Photovoltaics: Research and Applications*, Vol. 21, No. 4, pp. 620–630.

Inmet, 2022. "Banco de dados meteorológicos - curitiba". URL `https://portal.inmet.gov.br/dadoshistoricos`.

Islam, M., Pandey, A., Hasanuzzaman, M. and Rahim, N., 2016. "Recent progresses and achievements in photovoltaic-phase change material technology: a review with special treatment on photovoltaic thermal-phase change material systems". *Energy Conversion and Management*, Vol. 126, pp. 177–204.

Jebasingh, E.B., 2016. "Effects of various types of graphite on the thermal conductivity and energy storage properties of ternary eutectic fatty acid-based composite as phase change material". *Renewables: Wind, Water, and Solar*, Vol. 3, No. 1, pp. 1–6.

Malvi, C., Dixon-Hardy, D. and Crook, R., 2011. "Energy balance model of combined photovoltaic solar-thermal system incorporating phase change material". *Solar Energy*, Vol. 85, No. 7, pp. 1440–1446.

Mau, S. and Jahn, U., 2006. "'performance analysis of grid-connected pv systems". *Arsenal Res., Bus. Area Renew. Energy Technol., Vienna, Austria, Tech. Rep. IEA-PVPS*, Vol. 2, p. 2006.

Osaka, W.G., 2019. *proposta de sistema fotovoltaico-térmico com material de mudança de fase para a melhoria da eficiência energética*. Ph.D. thesis, Pontifícia Universidade Católica do Paraná.

Pereira, E.B., Martins, F.R., Gonçalves, A.R., Costa, R.S., Lima, F.L., Rüther, R., Abreu, S.L., Tiepolo, G.M., Pereira, S.V. and Souza, J.G., 2017. "Atlas brasileiro de energia solar - 2 ed". *São José dos Campos: INPE*, p. 80.

Rad, M.A.V., Kasaeian, A., Mousavi, S., Rajaee, F. and Kouravand, A., 2021. "Empirical investigation of a photovoltaic-thermal system with phase change materials and aluminum shavings porous media". *Renewable Energy*, Vol. 167, pp. 662–675.

Sarı, A., Biçer, A., Karaipekli, A., Alkan, C. and Karadag, A., 2010. "Synthesis, thermal energy storage properties and thermal reliability of some fatty acid esters with glycerol as novel solid–liquid phase change materials". *Solar Energy Materials and Solar Cells*, Vol. 94, No. 10, pp. 1711–1715. ISSN 0927-0248.

Sharma, A., Tyagi, V.V., Chen, C.R. and Buddhi, D., 2009. "Review on thermal energy storage with phase change materials and applications". *Renewable and Sustainable energy reviews*, Vol. 13, No. 2, pp. 318–345.

Stoffel, T. and Andreas, A., 2006. "Nevada power: Clark station; las vegas, nevada (data)". Technical report, National Renewable Energy Lab.(NREL), Golden, CO (United States).

Zhao, C., Wang, J., Sun, Y., He, S. and Hooman, K., 2022. "Fin design optimization to enhance pcm melting rate inside a rectangular enclosure". *Applied Energy*, Vol. 321, p. 119368. ISSN 0306-2619.

7. RESPONSIBILITY NOTICE

The authors are solely responsible for the printed material included in this paper.